Proc Indian Natn Sci Acad, **70, A,** No.1, January 2004, pp.53–61

SURVEY OF EXPERIMENTS WITH REACTOR NEUTRINOS*

C V K BABA
Nuclear Science Centre, New Delhi-110067 (India)

(Received 10 February 2003; Accepted 30 June 2003)

Beginning with the very first detection of the electron anti-neutrino by Reines and Cowan, reactor neutrinos have played an important role in our understanding of the properties of the neutrinos. This article summarises the recent experiments with reactor neutrinos which is now in a decisive phase.

Key Words: Reines-Cowan Experiment; Spectrum of Reactor Neutrinos; Bugey Experiment; CHOOZ Experiment; KamLAND Experiment

1 Introduction

While the existence of a neutrino (ν) was postulated in 1930 by Pauli, the experiments on/with it could start only after an experimental verification of its existence in 1953 by Cowan and Reines[1], via the reaction $\bar{\nu}_e + p \rightarrow e^+ + n$. Davis[2] could not observe the reaction $\bar{\nu}_e + {}^{37}Cl \rightarrow e^- + {}^{37}Ar$, while this could be observed with neutrinos from the Sun. Thus it was shown very early that in the inverse β decay reactions ν_e's can result in e^- whereas $\bar{\nu}_e$ will result in the production of e^+. Since then several types of neutrinos and anti-neutrinos have been identified ($\nu_\mu, \bar{\nu}_\mu, \nu_\tau, \bar{\nu}_\tau$) and experiments with some of them have become possible. Among extra-terrestrial sources are the solar neutrinos (ν_e up to about 15 MeV in energy), relic neutrinos (of all types), neutrinos from supernovae (of energies up to tens of MeV), neutrinos produced by cosmic rays (atmospheric neutrinos of all types up to tens of GeV and even above), and all of these except the relic neutrinos have been detected and important physics insights have been obtained, for example, neutrino properties, solar neutrino problem, atmospheric neutrino anomaly and their explanation in terms of neutrino oscillations. Among the terrestrial sources are the neutrinos associated with naturally occuring beta emitters inside the Earth, and the laboratory sources like reactors, neutrinos resulting from the decays of particles produced at accelerators and strong beta-radioactive sources. Experiments with these sources also have been helpful in the understanding of neutrino physics.

For a complete understanding of neutrino physics it is necessary to do experiments with all these sources of neutrinos. In this article we shall discuss some of these experiments that have been conducted with $\bar{\nu}_e$'s from nuclear reactors. There have been two excellent reviews recently on this topic[3,4]. Reactors are copious sources of electron antineutrinos $\bar{\nu}_e$ of energies up to a few MeV. Some of the salient features of these experiments are:

1. Since these experiments are with $\bar{\nu}_e$ they are, in principle, different from experiments with ν_e, for example from the Sun, and can be useful in testing CPT and CP violations.

2. Most of the reactor neutrino experiments use the reaction

$$\bar{\nu}_e + p \rightarrow n + e^+. \qquad \ldots(1)$$

These experiments are insensitive to the possible production of $\bar{\nu}_{\mu,\tau}$ as a result of oscillations since the charged current interactions of these to produce μ, τ are energetically not possible due to the low energy of reactor anti-neutrinos. Thus only disappearance or depletion experiments (reduction of $\bar{\nu}_e$ flux) are possible.

3. Solar neutrino experiments showed a reduction of ν_e's expected on the basis of the Standard Solar Model (SSM). Similarly the atmospheric neutrinos also showed a deficit in the

* This article is based on a talk given at Neutrino-2001 at The Institute of Mathematical Sciences in Chennai. The information contained in this article is compiled from original sources by the author and is not based on original research.

expected flux of muon neutrinos and muon-anti-neutrinos. These experiments have been interpreted in terms of neutrino oscillations among the three flavour eigenstates[5]. These flavour eigenstates are mixtures of three neutrinos ν_1, ν_2, ν_3 of masses m_1, m_2, m_3. The parameters that enter any neutrino oscillation model are the two mass-squared differences $\delta_{12} = |m_2^2 - m_1^2|, \delta_{23} = |m_3^2 - m_2^2|$ and the three mixing angles $\theta_{12}, \theta_{13}, \theta_{23}$ that characterise the mixing between the three pairs of states. The atmospheric neutrino anomaly indicated a δ in the region $10^{-3} - 10^{-2}$ eV^2 and the solar neutrino problem points to a δ of $10^{-5} - 10^{-4}$ eV^2 showing that there are two distinct mass scales. For the case of vacuum oscillations the survival probability $P_S(\bar{\nu}_e \to \bar{\nu}_e)$ of an original electron antineutrino of energy $E_{\bar{\nu}}$ after travelling a distance L is given by[5]

$$\begin{aligned} P_S &= 1 - \cos^4(\theta_{13})\sin^2(2\theta_{12})\sin^2(\varepsilon_{12}) \\ &\quad - \sin^2(2\theta_{13})[\cos^2(\theta_{12})\sin^2(\varepsilon_{13}) \\ &\quad + \sin^2(\theta_{12})\sin^2(\varepsilon_{23})] \qquad \ldots(2) \end{aligned}$$

where ε_{ij}'s give the energy dependence of P_S with

$$\varepsilon_{ij} = \frac{1.27\delta_{ij}(eV^2)L(meters)}{E_{\bar{\nu}}(MeV)}. \qquad \ldots(3)$$

One can see that the sensitivity of a depletion experiment depends on ε_{ij} since this factor should be of the order of unity for a measurable energy dependent depletion. This expression can be further simplified if there is a hierarchy among masses such that $\delta_{12} << \delta_{13} \approx \delta_{23}$[5]. Such a hierarchy is suggested by the two mass scales that we mentioned already. With this proviso the survival probability is given by

$$\begin{aligned} P_S &= 1 - \cos^4(\theta_{13})\sin^2(2\theta_{12})\sin^2(\varepsilon_{12}) \\ &\quad - \sin^2(2\theta_{13})\sin^2(\varepsilon_{13}). \qquad \ldots(4) \end{aligned}$$

For reactor neutrinos ($E_{\bar{\nu}} \approx$ few MeV) ε_{1j} is significant only for δ_{ij} in the range $10^{-3} - 10^{-2}$eV^2 for L of the order of 1 km. While for L of the order of 100 km, δ_{ij} in the range $10^{-5} - 10^{-4}$eV^2 gives observable effects for reasonably large mixing angles. If one identifies δ_{13} with the first range and δ_{12} with the second one can see $L \approx 1$ km experiment is sensitive to the third term in the above equation while $L \approx 100$ km experiment is also sensitive to the second term so that a combination of the results of both these experiments can lead to a better understanding of the oscillation problem. As shown later the CHOOZ and Palo Verde (L around 1km) and KamLAND (L around 180 km) accomplish this. Thus even among reactor experiments one can get complementary information from experiments with different baselines. Further, we can see from the above expressions that several experiments with neutrinos of various energies are required to get complete determination of parameters in neutrino oscillation models.

4. Other experiments with reactor antineutrinos leading to further understanding of neutrino physics are possible if detectors using different reactions, especially those having low detection threshold are used (see later).

2 Reactor Antineutrinos and their Detection

Most, if not all, of the reactor $\bar{\nu}_e$ experiments need a knowledge of the flux and the energy spectrum as inputs. For example, the depletion experiments measure the spectrum and flux at a given distance from one or more power reactors and depend on a knowledge of the original energy dependent antineutrino flux. The utility of these reactor experiments comes from the fact that the yield and the spectrum can be known to a good accuracy. Almost all the reactor experiments, especially those on neutrino oscillations, use the reaction (1) for their detection.

Flux and Energy Spectrum

In nuclear power reactors the antineutrinos are produced isotropically from the β^- decay of the fission fragments from the thermal neutron induced fission of ^{235,238}U, ^{239}Pu and ^{241}Pu. A simple estimate of the total $\bar{\nu}_e$ production rate can be made from the fact that the energy released per fission is about 200 MeV and the number of $\bar{\nu}_e$ is about 6 per fission. Using this fact the neutrino yield per second at the core is given by,

$$Y_{\bar{\nu}_e} = \frac{P_{th}(GW)6.24 \times 10^{21} \times 6}{200} \qquad \ldots(5)$$

which works out to 2×10^{20} $\bar{\nu}_e$'s per second at the core of a reactor with 1GW thermal power. This yield and the energy spectrum are slightly different for the four fissile nuclei mentioned above. They can be obtained either through calculations[6] or through empirical means[7].

In the first approach all the beta decay chains from the fission of each of the fissile nuclei are calculated. Combining these and the fission fragment distribution data the $\bar{\nu}_e$ spectrum can be calculated. The uncertainties in such calculations are mainly due to the unknown decay schemes of short lived fission fragments.

In the empirical approach the β^- spectrum from fission of each of the fissile nuclei, continuously bombarded by thermal neutrons, is measured, decomposed into a large number of β^- spectra with different end points and mean charge distributions assuming allowed β decays. From such a decomposition the $\bar{\nu}_e$ spectrum can be reconstructed. The β^- spectra were found not to change with time after about ten hours from the start of the thermal neutron irradiation, for β energies above a certain minimum energy reflecting the fact that the half lives of the activities that give rise to these β^-'s is less than a few hours. The absolute flux of β^- and hence $\bar{\nu}_e$ is also experimentally determined from neutron flux and target atom number measurements. The yield and flux for each of these fissile nuclei is slightly different. The relative abundances of these fissile nuclei evolve with the reactor running. This can be taken into account from a continuous data about the operating parameters of a reactor. The flux and spectrum calculated and empirically determined agree with each other to about one percent. It is thus estimated that the yield is known to an overall accuracy of about 1.5 percent[8].

Detection

Some of the convenient reactions that can be used to detect and measure $\bar{\nu}_e$ energy are listed in Table I below along with the threshold and an energy averaged cross-section per fission.

The energy dependent cross sections of the first four reactions in Table I are known to a very good accuracy up to about 2 percent. The most common reaction used especially in neutrino oscillation experiments is the first one using a liquid scintillator as a target. The reaction is identified by measuring a "prompt" signal due to the stopping and annihilation of e^+. The observed "prompt" energy ($T_{e^+} + 2m_e = E_{\bar{\nu}} - 0.8\text{MeV}$) leads to a measurement of the antineutrino energy. This prompt signal is to be followed by another signal generated by the neutron usually after thermalisation. This signal is delayed because of the slowing down time of the neutron in the detector, which is detected by observing a 2.2 MeV gamma ray following $n_{th} + p \rightarrow d + \gamma$ or a high energy (approximately 8 MeV) gamma ray from the neutron capture in a material with large thermal neutron cross section (usually Gd or Cd) loaded in the medium. Requirements on the position of the prompt and delayed signals and the delay between them help in the better identification of the event. Some experiments detect neutrons by measuring the charged particles produced in the neutron induced nuclear reactions like $n + {}^6Li \rightarrow \alpha + t$ and $n + {}^3He \rightarrow d + t$. A summary of some of the experiments with reactors using eq.1 is given in Table II.

Table I

Table showing various reactions for neutrino detection. The last two rows refer to neutrino excitation of nuclei via neutral and charged current reactions

Reaction	Threshold (MeV)	$<\sigma>$ (cm^2)/fission
$\bar{\nu}_e + p \rightarrow e^+ + n$	1.8	60×10^{-44}
$\bar{\nu}_e + d \rightarrow e^+ + n + n$	4.0	1.2×10^{-44}
$\bar{\nu}_e + d \rightarrow \bar{\nu}_e + p + n$	2.3	2.9×10^{-44}
$\bar{\nu}_e + e^- \rightarrow \bar{\nu}_e + e^-$		0.6×10^{-44} (for $T_e > 1$ MeV)
$\bar{\nu}_e + A \rightarrow e^+ A'$		
$\bar{\nu}_e + A \rightarrow \bar{\nu}_e + A'$		

3 Searches for Neutrino Oscillations at Nuclear Reactors

Searches for neutrino oscillations using reactor neutrinos by detecting a depletion started as early as in 1977[10]. Some of the experiments looked for a deviation of the flux from a $1/r^2$ dependence[11]. Such an approach does not need an exact knowledge of the absolute flux of the antineutrinos. As our understanding of the energy dependent flux became more precise, most of the later experiments relied on a comparison between the measured and calculated fluxes. None of the experiments, with the exception of the recent KamLAND, could detect a depletion and could obtain upper limits on the mixing parameters. Such limits, however have been very valuable for example in limiting the value of θ_{13}. Recent experiments are long baseline experiments and are often done underground to reduce backgrounds. The improvement in the quality of the experiments can be gauged from Table II. A

Table II
Summary of the reactor neutrino experiments around the world

Experiment (year)	depth (MWE)	Power /Flux	Distance	Mass (Tons)	Overall Eff.	Rates signal(bkg)
Hanford[1] (1953)	surface			0.3		0.4/min (2.0/min)
Savannah[9] 1956-59	surface	$10^{13}/cm^2/s$		2×0.2	0.26/hr	3/hr(0.6/hr)
ILL[10] 1977	surface	$10^{12}/cm^2/s$	9 m		0.194	1.6/hr(1/hr)
Goesgen[11] 1985	surface		40-60m	0.4	0.167	1.5-4/hr(1.8/hr)
Bugey[12] 1995	surface	2.8 GWth	15-95 m	3×0.6	0.42	63-1.4/hr(2-7/hr)
CHOOZ[13] 1997-99	300	8.5GWth	1.1 km	5	0.698	25/day(1.2/day)
Palo Verde[14] 1998-99	32	11.6 GWth	0.8 km	11	0.1	20/day (25/day)
KamLAND[15] 2001-	2700	130 GWth	180 km	1000	0.78	2.3/day (0.1/day)

brief description of some of the typical experiments is given below.

Bugey Experiment

This experiment was done at several distances (15 to 90 m) from 2.8 GWth reactors at Bugey[12], using three detectors of 600 litres each. Each of these detectors/targets was segmented into 98 cells and consisted of 0.15% ^{6}Li loaded scintillator. The scintillations in each of these cells were isolated and viewed by three photomultipliers. The neutron after thermalisation was detected by the $n + {}^6Li \rightarrow \alpha + t$ reaction, the α and t being identified in the scintillator by pulse shape detection techniques. From a comparison of fluxes at several distances limits on δ of $0.05 - 0.01$ eV^2 were placed for a maximally mixed two flavour scenario.

The CHOOZ and Palo Verde Experiments

The CHOOZ experiment was set up at a site near two pressurized light water moderated nuclear reactors with a total thermal power of 8.5 GWth. The detector[13] was located at a distance of about 1 km from each of the reactors with about 300 m water equivalent of rock overburden to reduce the cosmic ray muon flux by 300 to 0.4 m^{-2} sec^{-1}.

The detector (see Fig.1) consists of a Gd-loaded (0.09%) 5 ton liquid scintillator placed in a transparent plexiglass container which acts as a neutrino target.

An intermediate region with about 17 tons of unloaded liquid scintillator (0.7 m thick) viewed by 192 twenty cm diameter photomultiplier tubes (PMT), shields the target from PMT radioactivity and contains

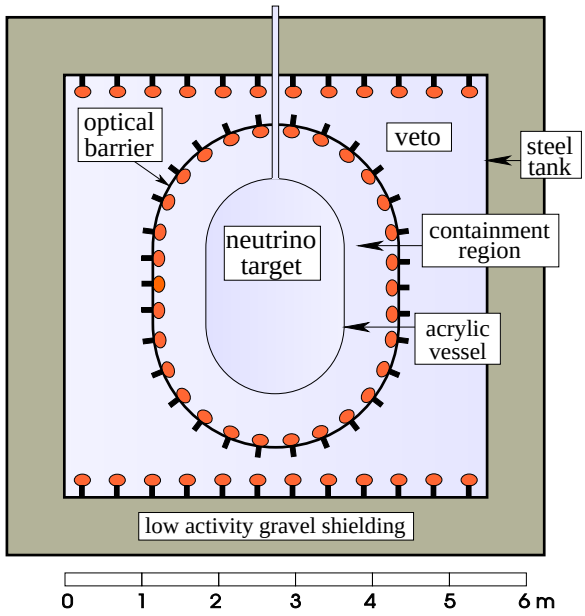

Fig. 1 The CHOOZ detector. The neutrino target consists of a 5 ton 0.09% Gd loaded liquid scintillator. The containment region consists of 17 ton liquid scintillator. Surrounding these is a 90 ton active muon veto shield. Figure taken from ref. [13].

the high energy gamma rays produced during the capture of thermal neutrons in Gd.

An outermost region which is optically isolated from the inner two regions consisting of 90 tons of scintillator (0.8 m thick) viewed by 48 twenty cm diameter PMTs provides an active cosmic ray veto signal.

The antineutrinos were detected through the reaction shown in eq.1. The experiment requires a delayed coincidence between a 'prompt' signal with en-

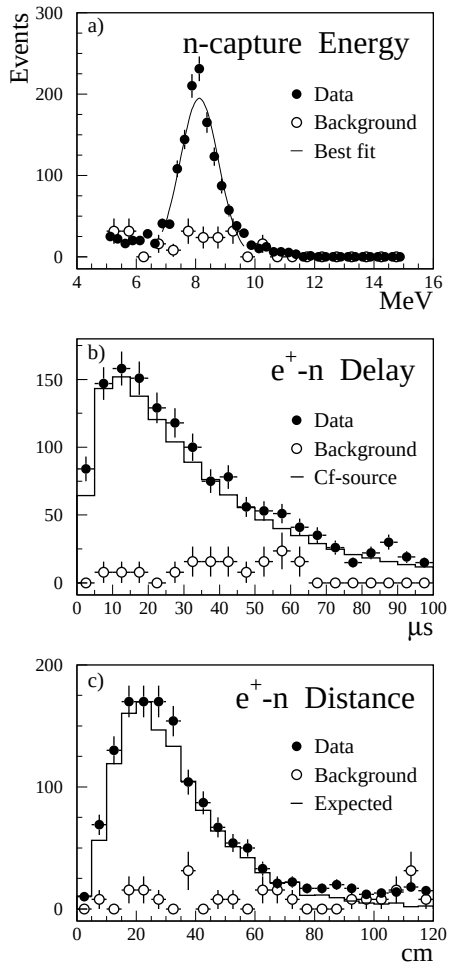

Fig. 2 (a) Distribution of energy release in n-capture on Gd. (b) Distribution of time delay between the prompt and secondary signals. (c) Distribution of distances between e^+ and n. The histograms indicate Monte-Carlo estimates.

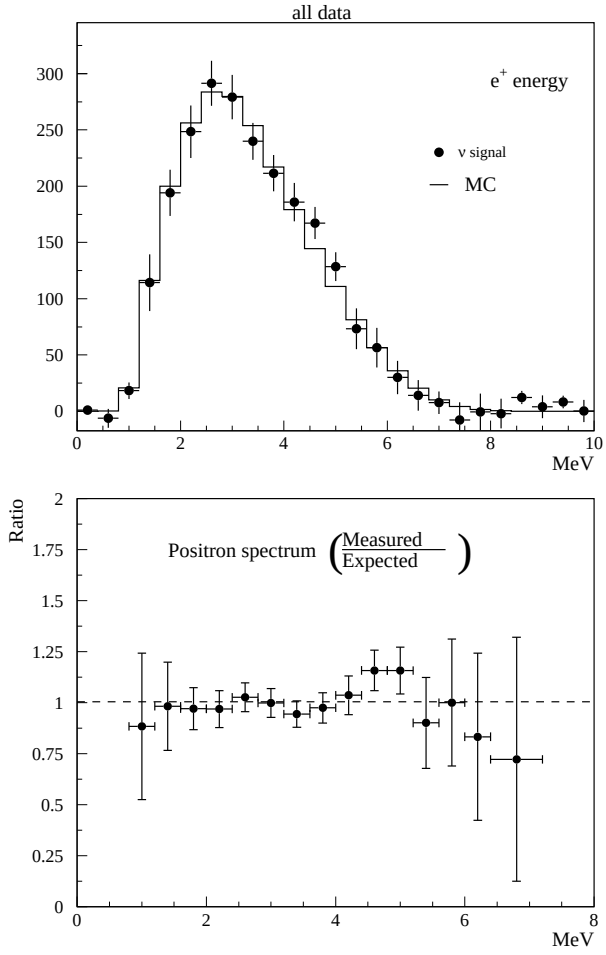

Fig. 3 (above): the measured background corrected 'prompt' energy spectrum in the CHOOZ experiment together with a histogram of the expected spectrum with no oscillation; (below): ratio of measured to expected spectra.

ergy deposit 1.3 - 8 MeV and another, a 'secondary' signal, with energy deposit 6 - 12 MeV within 2 - 100 μsec., and a spatial correlation to within a meter of each other. The former includes events with a stopping positron and leads to a determination of the prompt energy and the latter aims at emphasizing the neutron capture gamma ray signal following its thermalization. The neutron response was measured using a ^{252}Cf source placed at the center of the detector. The peaks arising from the neutron capture on hydrogen (2.2 MeV) and on Gd (8 MeV) were used to calibrate the detector. Typical energy resolutions at these two energies were 9% and 6%, respectively. The overall detection efficiency was found to be (69.8$\pm$1.1)%. Distributions of the energy released by neutron capture, the $e^+ - n$ time and spatial correlations are shown in Fig.2. Since the reactors came on line after the detector was ready the neutrino event rate- reactor power correlation could be seen. After selecting events based on the energy, time and position criteria, the positron energy spectra were generated. The final background corrected spectrum is shown in Fig.3. The calculated no oscillation and measured spectra agree with each other fairly closely. The energy averaged ratio of the measured to calculated neutrino signal is 1.01$\pm$ 0.028 (stat)$\pm$ 0.027 (syst).

A similar experiment was performed[14] at 0.8 km from the power reactors at Palo Verde with a combined thermal power of 11.6 GWth, using 11.3 tons of 0.1% GD loaded liquid scintillator, segmented into 6×11 array of 9 meter long cells viewed at both ends by 12.7 cm dia photomultipliers to reduce the cos-

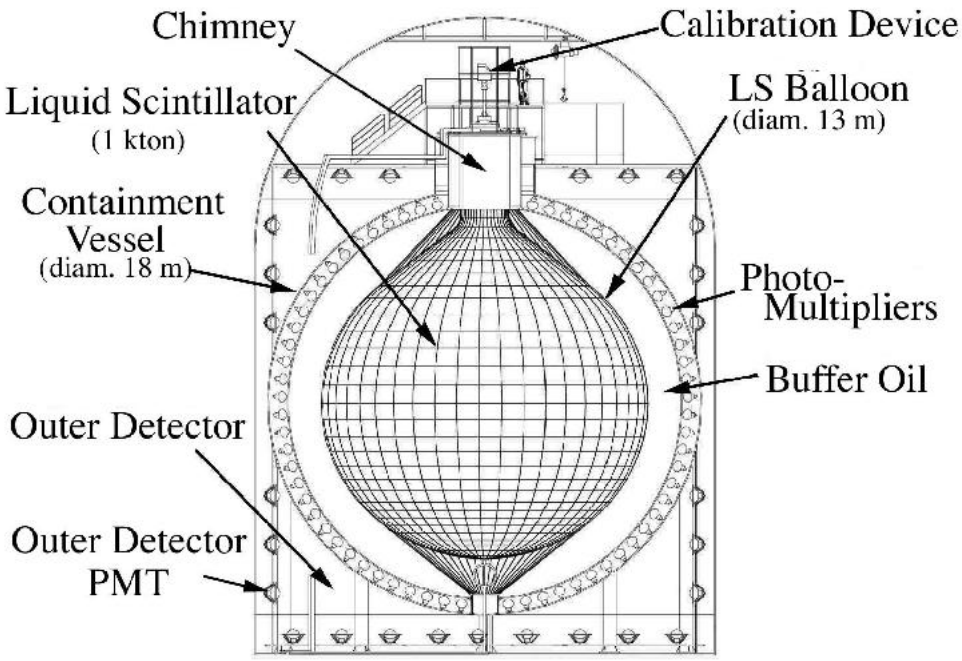

Fig. 4 A schematic diagram of the KamLAND detector from ref. [15]

mic ray backgrounds which were considerably larger than in the CHOOZ experiment. The overall detection efficiency was about 0.1. The energy averaged ratio of the measured to calculated neutrino signal is 1.01±0.024(stat)±0.053(syst).

Combining the results of the CHOOZ and Palo Verde experiments with the solar neutrino results, allowed regions of δ and $\sin^2(2\theta)$ have been determined in two flavour oscillation scenarios[4]. However, the importance of these results is evident if we consider the simplified expression in the three flavour case, as given by eq.4. As mentioned earlier, the depletion for these experiments mainly comes from the term $\sin^2(2\theta_{13})\sin^2(\varepsilon_{13})$. The measured upperbounds on depletion from these experiments have placed limits on $\sin^2(2\theta_{13}) < 0.15$. It has not been possible to obtain such a limit from other experiments. There are even some proposals for similar experiments[16] so as to obtain better limits on θ_{13}.

The KamLAND Experiment

The KamLAND experiment[15] is a long baseline experiment searching for neutrino oscillations with a sensitivity for large mixing angles to δ in the range 10^{-5} eV^2 to 10^{-4} eV^2 (δ_{12}) since the L/E in this case is in the range 10^5 to 10^4 m MeV^{-1} (see eq.3). The experiment located at Kamioka in Japan with a rock overburden of about 1 km, consists of 1 kT liquid scintillator (see Fig.4) of ultra-high purity, detecting antineutrinos from the surrounding nuclear power reactors (numbering 51 with total power 130 GWth) at distances between 130 and 220 km. The U/Th and ^{40}K impurities in the scintillator are of the order of a few parts in 10^{16} while the radon impurity gives an activity of about 4 Bq/m^3. This is surrounded by a 2.5 m thick mineral oil shielding. These are placed in a 18 m diameter stainless steel spherical container with 2000 PMTs of 43 and 50 cm diameter on the inside viewing the scintillator. This gives a photocathode coverage of about 30%. Outside the stainless steel container is a tank of 3.2 kiloton water-Cherenkov detector, viewed by 225 25cm dia PMT's to veto cosmic ray events. The PMT signals are digitized by analog transient waveform digitizers. This helps in discriminating the alpha background from U/Th/Rn activities through pulse shape discrimination. The fast time response of the scintillator is used to get a position information from the relative times of the PMTs firing. The position resolution is about 25 cm (FWHM). The energy resolution of the liquid scintillator detector is approximately $7.5\%/\sqrt{E\,(MeV)}$. The antineutrino events were selected on the basis of cuts in the fiducial volume, time and position correlations between the 'prompt' and delayed or secondary signals produced by n-capture on hydrogen after thermalisation. The overall efficiency was (78.3±1.6)%.

The background corrected 'prompt' energy spec-

trum obtained in a 145 day run (corresponding to an overall exposure of 162 ton-yr), together with a calculated no oscillation spectrum are shown in the lower part of Fig.5. An energy dependent depletion of antineutrinos in a reactor experiment has been observed for the first time in this experiment. An energy averaged (for $E_{\bar{\nu}_e} > 3.4$ MeV) ratio of the measured events to those calculated in the absence of oscillations was found to be $0.611 \pm 0.085(\text{stat}) \pm 0.04(\text{syst})$.

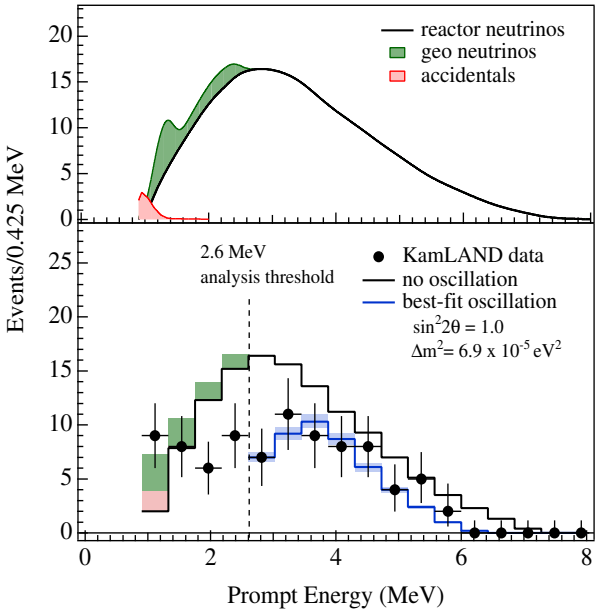

Fig. 5 Top: Expected 'prompt' energy spectrum due to antineutrinos from the reactor and background sources at the KamLAND detector. The lower panel shows a histogram of the measured 'prompt' spectrum along with one expected in the absence of oscillations. The lower histogram in the lower panel shows the best fit with oscillations.

The data of this experiment together with those of earlier ones was analysed in a two flavour scenario to yield a value of $\delta \approx 6.9 \times 10^{-5}\text{eV}^2$ and $\sin^2 2\theta = 1.0$ (see ref. [15] and the plot in Fig.6). For the conditions of the KamLAND experiment, eq.4 approximates to

$$P_S \approx \cos^4\theta_{13}[1 - \sin^2 2\theta_{12}\sin^2\varepsilon_{12}]. \quad \ldots(6)$$

With the limit $\sin^2 2\theta_{13} < 0.15$[13], the KamLAND result leads to $0.86 \leq \sin^2 2\theta_{12} \leq 1.00$.

The observed depletion in the KamLAND experiment singles out the so-called Large Mixing Angle solution to the solar neutrino problem if CPT invariance is assumed. It is expected that more data from KamLAND will result in more precise values for the mixing parameters.

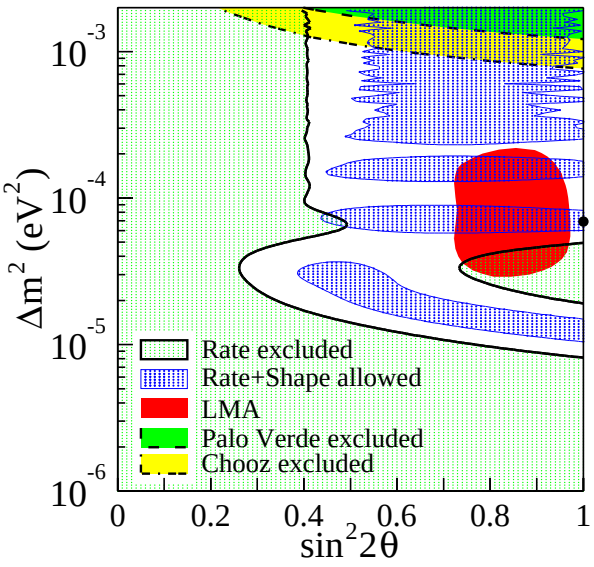

Fig. 6 Excluded and allowed regions in the δ (shown as Δm^2 in the figure) and $\sin^2 2\theta$ from the various reactor based antineutrino oscillation experiments. The allowed LMA(large mixing angle) solution from the solar neutrino analysis is also indicated. The thick dot indicates the best fit to the KamLand data. The 95% confidence level allowed regions from KamLAND are also shown. Figure taken from ref. [15]

4 Magnetic Moment of the Antineutrinos

As has been mentioned earlier, additional antineutrino properties can be obtained if the experiments can be performed at lower energies. In addition to establishing bounds on the (anti)neutrino magnetic moment, reactor experimental searches for decay of heavier neutrinos have been performed. Again bounds have been established on the decay rates[17]. Apart from its effect on the solar neutrino problem, the existence of a magnetic moment for neutrino is of great fundamental importance (for example, μ_ν is possible only if the mass is nonzero). Several experiments have already placed upper limits on $\mu_{\bar{\nu}}$ in the region $2 - 4 \times 10^{-10}\mu_B$[18]. One of the possible ways of measuring the magnetic moment is through the energy dependence of $\nu_e - e$ elastic scattering, since the amplitude for this scattering has a different energy dependence from that due to weak interaction. This cross section as a function of the recoil energy T of the elec-

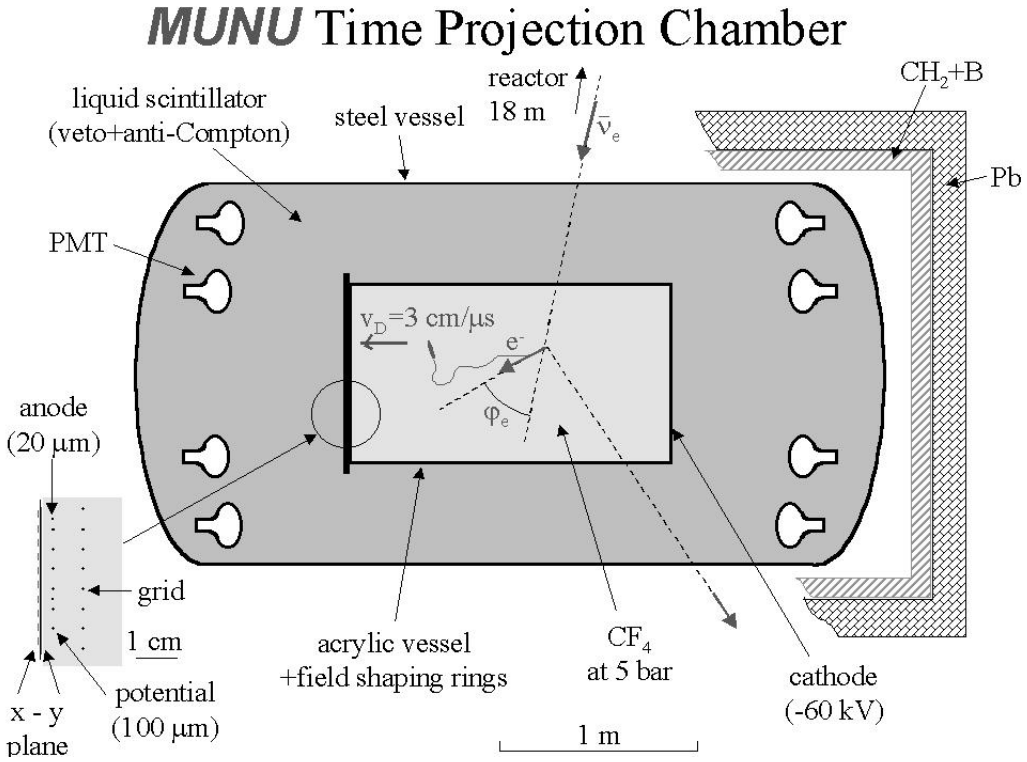

Fig. 7 A schematic view of the arrangement of the MUNU experiment. It measures the recoil energy and angle of the electron following antineutrino-electron elastic scattering

tron for an incident energy $E_{\bar{\nu}}$ is given by[19]

$$\frac{d\sigma}{dT}(\bar{\nu}_e - \bar{\nu}_e) = \frac{2G_F^2 m_e}{\pi}\left[g_R^2 + g_L^2(1-\frac{T}{E_{\bar{\nu}}})^2 - g_L g_R \frac{m_e T}{E_{\bar{\nu}}^2}\right] + \frac{\pi\alpha^2\mu_{\bar{\nu}_e}^2}{m_e^2}\frac{1-T/E_{\bar{\nu}}}{T} \quad \ldots(7)$$

where $g_R = \sin\theta_w, g_L = g_R + 1/2$ and G_F is the Fermi coupling constant. The second term containing the fine structure constant α is due to the magnetic moment of the $\bar{\nu}_e$. It can be seen that for $\sin\theta_w = 0.23$ and $E_{\bar{\nu}} \approx m_e$ the first term vanishes for backward scattering since $T/E_{\bar{\nu}} = 2/3$. Thus a measurement of this cross section at backward angles (forward recoiling electron) for $E_{\bar{\nu}}$ around m_e is very sensitive to the magnetic moment $\mu_{\bar{\nu}_e}$ (see ref. [20]).

The experiment MUNU has been setup at the Bugey reactor to measure the magnetic moment of the antineutrino. The detector (see Fig.7) is placed about 18 meters from the core of the power reactor (2.7 GWth) and consists of a time projection chamber filled with CF_4 gas at 5 bar pressure. The X-Y position information of the recoiling electron subsequent to a $(\bar{\nu}_e, e)$ elastic scattering event is recorded via the signals on the anode plane in addition to the drift time which gives the Z information. The energy spectrum of the recoiling electrons from, (ν_e, e) elastic scattering will be used constrain the magnetic moment of the antineutrino. Preliminary results[21] from MUNU give an upper limit of 1.5 x 10^{-10} μ_B on the magnetic moment of the electron antineutrino.

The Texono collaboration[22] uses a high purity germanium detector in a low background environment to search for an excess of low energy scattering events arising from antineutrino scattering due to a possible magnetic moment. The first results place an upper limit of 1.5 x 10^{-10} μ_B on the magnetic moment of the electron antineutrino[22].

5 Conclusions

Since the first experiments in 1953 that lead to the experimental discovery of the (anti)neutrino, nuclear reactor based neutrino experiments have provided us with a wealth of information. In recent years such experiments have complimented other neutrino experiments at high energies. Some of the on-going experiments like the KamLAND will help in precise determination of the oscillation parameters. Additional properties of the (anti)neutrino like a possible magnetic moment are expected to be understood as a re-

sult of some of the on-going and planned experiments at nuclear reactors, using various types of detectors, especially at low energies.

The author wishes to thank V M Datar, M V N Murthy and D Indumathi for extensive help in the preparation of the manuscript.

References

1 F Reines, C L Cowan Jr. *Phys Rev* **92** (1953) 830

2 R Davis Phys Rev **97** (1955) 766

3 F Boehm Studies of Neutrino Oscillations at Reactors *Current Aspects of Neutrino Physics* (Ed. David Caldwell) Springer-Verlag Heidelberg (2001)

4 C Bemprad, G Gratta and P Vogel *Rev Mod Phys* **74** (2002) 297

5 See for example the review by A Raychaudhuri in this volume

6 P Vogel *et al Phys Rev* C **24** (1981) 1543

7 K Schreckenbach *et al Phys Lett* B **160** (1985) 325

8 Y Declais *et al Phys Lett* **B338** (1994) 383

9 F Reines and C L Cowan Jr. *Nature* **178** (1956) 446

10 F Boehm, J F Cavaignac, F V Feilitsch, A Hahn, H E Henrikson, D H Koang, H Kwon, R L Mossbauer, B Vignon and J L Vuilleumier *Phys Lett* B **97** (1980) 310; H Kwon *et al Phys Rev* D**24** (1981) 1097

11 G Zacek *et al Phys Rev* D**34** (1986) 2621

12 B Achkar *et al Nucl Phys* B**434** (1995) 503

13 M Apollonio *et al Phys Lett* B**420** (1998) 397; *ibid* B **466** (1999) 415

14 F Boehm *et al Phys Rev Lett* **84** (2000) 3764

15 K Eguchi *et al* KamLAND Collaboration *Phys Rev Lett* **90** (2003) 021802

16 L Mikaelyan *et al Nucl Phys (Proc Suppl)* **B91** (2001) 120

17 J Boucher *et al Phys Lett* **B207** (1988) 217; S Schoenert *et al Nucl Phys (Proc Suppl)* **B48** (1996) 201

18 C L Cowan and F Reines *Phys Rev* **107** (1957) 528

19 P Vogel and J Engel *Phys Rev* D **39** (1989) 3378

20 J Segura, J Bernabeu, F J Botella and J Penarrocha *Phys Rev* D**49** (1994) 1633

21 M Avenier *et al Nucl Instrum Meth* **A482** (2002) 408

22 J Vuilleumeir (Talk presented at Neutrino 2002 http://neutrino2002.ph.tum.de/)